

# FAMCAR Approach for Efficient Multi-Carrier Ambiguity Estimation

Ulrich Vollath, *Trimble Terrasat GmbH*  
Knut Sauer, *Trimble Terrasat GmbH*

## BIOGRAPHY

Dr. Ulrich Vollath received a Ph.D. in Computer Science from the Munich University of Technology (TUM) in 1993. At Trimble Terrasat - where he is working on GPS algorithms since more than eleven years - he is responsible for the Algorithm Development team. His professional interest is focused on high-precision real-time kinematic positioning and reference station network processing.

Dr. Knut Sauer received a Ph.D. in Satellite Navigation from the Imperial College of Science, Medicine and Technology, London. 2003 he joined Trimble Terrasat as software and development engineer where he is working on high precision kinematic positioning using the future Galileo system.

## ABSTRACT

The proposed addition of a third carrier for the modernized GPS as well as providing three and possibly four carriers for the planned Galileo system will boost the performance of carrier phase based positioning within the next decade. In principle, instantaneous (one-epoch) ambiguity resolution becomes feasible for a broad range of applications.

Beyond the system level developments - regarding the frequency allocation and signal structure - the proposal of three and four carrier frequencies enables new approaches at the processing level.

The Factorized Multi-Carrier Ambiguity Resolution (FAMCAR) algorithm introduces a number of new independent linear combinations of carrier-phase observations as well as of carrier-phase and pseudo-range observations. The combinations include the minimum-error geometric carrier-phase combination, the minimum-error ionosphere combination, the new Quintessence combinations and the code-carrier combinations. From these individual estimates, the full floating solution for all carriers is derived.

The paper will give a description of the approach and the statistical properties of these new linear combinations. Results of an experiment using FAMCAR for hardware-simulated data are presented in another paper.

Existing standard techniques for multi-carrier ambiguity determination usually apply one big Kalman filter to estimate all unknowns (e.g. position, ambiguities, ionosphere and multipath). The factorization enables the stepwise modeling of each error component and leads therefore to a bank of significantly smaller filters. This approach results in significantly higher computational efficiency for the Kalman filter sets (i.e. float solution) and a better knowledge of error components for the individual measurements. In addition to enabling efficient processing of three and four carrier data the new approach is already applicable to a dual-frequency system. Furthermore the decreased computational load enables the use of smaller processor components and therefore provides a significant cost reduction.

## INTRODUCTION

In the past years, starting with an existing technique a new and very efficient ambiguity resolution algorithm has been developed. Focusing on temporally correlated error sources like multipath and ionosphere, a solution was sought to handle these without sacrificing computational efficiency. These advances processing techniques were first implemented for two carriers in the Trimble Total Control 2.7 post-processing package. The extension to three and more carriers was implemented to provide a powerful and efficient processing method to an analysis experiment.

To emulate performance analyses near to reality, a hardware simulation of the new signals was performed under an ESA/ESTEC contract. This project is the follow-up of experiments investigating three-carrier ambiguity resolution ([Vollath et. al. 1998], [Vollath et. al. 2001]). The main purpose of the experiment was to investigate if the benefits of a fourth carrier justify a commercial pay-service. Also, differences in the expected performance of modernized GPS and Galileo were of interest.

Another paper submitted to this conference ([Sauer et. al. 2004]) gives a brief overview on the actual experiment performed at the European Space and Technology Centre (ESTEC).

This paper starts with overviews of ambiguity resolutions techniques, and especially the ones designed for use with the new three (and more) carrier GNSS.

The importance of modeling temporally correlated errors is stressed in the next paragraph.

Next, a first approach for a factorized solution is presented. The extension of this starting point to a completely decentralized approach is the central topic of this paper.

Statistical and computational properties of this new ambiguity resolution algorithm are given finally, justifying the approach as a valid, effective and enabling technique.

### AMBIGUITY RESOLUTION ALGORITHMS

Various algorithms exist for the resolution of the carrier-phase ambiguities. Despite all their differences, some properties can be given that are common for many of them. The differences are articulated in all steps of the complete ambiguity resolution process (Figure 1).

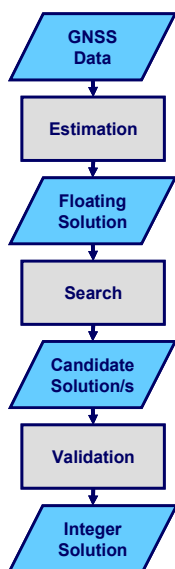


Figure 1: Ambiguity Resolution Process

The main steps in ambiguity resolution and their variations are:

#### Estimation (Float Solution)

Typically using some sort of least-squares adjustment, ambiguities are estimated not accounting for their integer nature. The computation of the floating solution can be done geometry-free or accounting for the geometry. Error sources can be modeled differently (see below).

#### Search

The best candidates for integer ambiguities are computed from their floating counterpart.

Bootstrapped algorithms or strict Integer Least Squares are used here or variants thereof.

#### Validation

The best solution is validated, i.e. it is verified that with a high probability the *best* solution is also the *correct* solution. Common tests are: ADOP-Test, Ratio-Test, Fisher-Test and other tests ([Teunissen et. al. 1997], [Wang et. al. 1998]).

The main focus of this paper is on the estimation part and the modeling of the errors.

### THREE-CARRIER AMBIGUITY RESOLUTION

Since the discussions of designing Galileo for three carriers ([Hein et. al. 2004]) and adding a third frequency to GPS ([Claiett 2003]), various proposals have been made on how to use this additional information. Among the basic proposals, the first TCAR (Three Carrier Ambiguity Resolution) algorithm has been presented by R.A. Harris ([Harris 1997], [Forsell et. al. 1997]).

Figure 2 shows the relation of some well-known algorithms to the categories presented before.

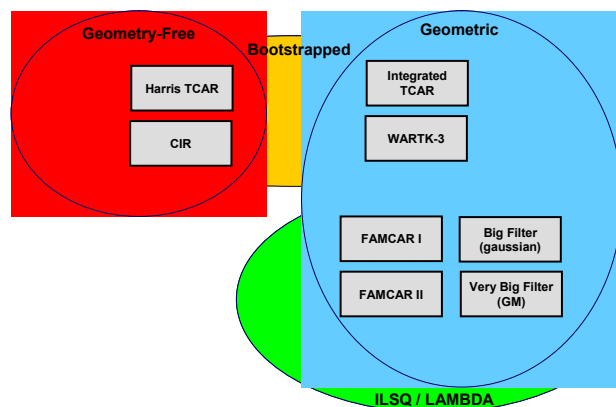


Figure 2: Ambiguity Resolution Algorithms

#### Harris TCAR/CIR

In 1997 a bootstrapped ambiguity resolution was proposed that resolved the ambiguities for three carriers in three steps using the so-called extra-widelane, widelane and L1 carrier phases ([Harris 1997], [Forsell et. al. 1997]). As a bootstrapped ambiguity resolution algorithm, it fails to maximize the success rates. Defined totally geometry-free, it also doesn't make use of the geometric information. Though very simple, this method ignores problems with multipath and ionosphere, and is mainly for that reason not of much practical relevance. Instead, it was a starting point for multiple algorithms, including CIR (Cascaded Integer Resolution). Multiple improvements have been developed since. Today, the term TCAR comprises the general family of ambiguity resolution algorithms for three carriers.

### Integrated TCAR/WARTK-3

Derived from the first TCAR, Integrated TCAR addressed some fundamental problems of it. By including geometry information, the success rates are increased. Also, ionosphere is modeled at least to some extent as random walk. WARTK and WARTK-3 ([Hernández-Pajares et. al. 2003]) are derived from Integrated TCAR. Latter method adds externally derived topographic ionosphere models to the last TCAR step which is most vulnerable to ionosphere.

### FAMCAR I

In a next evolution step, a full integer least squares search is implemented. The recommended efficient search method is LAMBDA here. Full use of geometry is made by the floating solution consisting of geometry and a geometry-free part (details below).

### FAMCAR II

The topic of this paper, this step extended FAMCAR with stochastic modeling of multipath and ionosphere. A very efficient floating solution set-up to enable full modeling is used (details below).

### “Big Filter” techniques

The complete observation equations are handled in one Kalman filter. Geometric and geometry-free information is not separated. Several degrees of multipath and ionosphere modeling are possible, from ignoring to complete modeling. This approach results in filters with many states, especially for many carrier frequencies.

### FACTORIZED MULTI-CARRIER AMBIGUITY RESOLUTION (FAMCAR)

During the TCAR-Test experiment funded by ESTEC ([Vollath et. al. 2001, I & II]), a first version of Factorized Multi-Carrier Ambiguity Resolution (FAMCAR) has been developed. The basic concept is separation of geometric and geometry-free information in the floating filter process, i.e. a federated filter approach ([Carlsson 1990]) for the floating solution.

In principle, the geometry filter determines the correlation between satellites by taking into account that the measurements refer to one common position. The geometry-free filters are independent between satellites and thus return the correlations between the ambiguities of the same satellite for different carriers.

The benefits are characterized by obtaining a better understanding of influences of signal structure (mainly affecting the geometry-free part) and geometry and introduction of efficiency as „enabling technique“. Due to the amount of data to be processed for analysis, tuning and final result processing, a fast processing option was necessary.

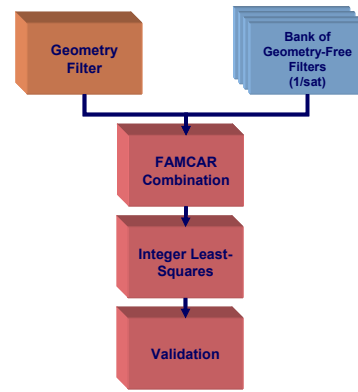


Figure 3: First FAMCAR technique

An overview of the first FAMCAR technique is given in Figure 3.

For this FAMCAR version, all errors considered Gaussian (multipath) or Random walk (ionosphere).

The consequential extension of the FAMCAR philosophy leads to the algorithm presented in this paper. In principle, separation of uncorrelated observables into different filters has been extended to a maximum.

### GM(1) MODELING

Among the different error sources present in GNSS signals, two are examined in more detail here: Multipath and ionospheric delay. Many models have been applied to these error sources, including no modeling (ignore the problem), Gaussian noise (ignoring the temporal correlation), constant bias (especially for ionosphere). Though not perfect, currently one of the best models for multipath is a first order Gauss-Markov process (GM(1)). For short observation periods and in lack of any physical modeling of the ionospheric layer, the same applies to ionosphere.

For Gaussian noise, the evolution of variances for  $n$  observations follows the formula

$$\sigma_{post}^2(n) = \sigma_0^2 \cdot \frac{1}{n}$$

This changes into

$$\sigma_{post}^2(n) = \sigma_0^2 \cdot \frac{1+r}{n-r(n-2)}; r = e^{-\frac{\Delta t}{t_{corr}}}$$

for GM(1) modeling with a time constant of  $t_{corr}$  and an update rate of  $\Delta t$ .

Figure 4 shows the example of a process consisting of a Gaussian noise component and a GM(1) process. The “Autocorrelation” graph shows the resulting autocorrelation function, having a peak at 0 seconds delay and dropping immediately to a value determined by the relation of correlated to total error.

After that, the typical exponential reduction of the correlation is shown. If this process is filtered assuming Gaussian noise only, the “Mismodeled Convergence” graph results, showing the relative improvement of a posteriori standard deviation over time. The correct implementation with Gaussian plus GM(1) errors (“True Convergence”) results in much higher (and realistic) a posteriori standard deviations.

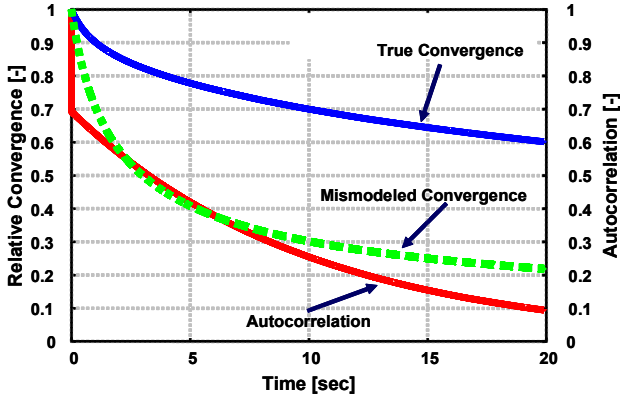


Figure 4: GM(1) process example with noise

One of the main problems with modeling these errors as noise is not so much the quality of estimation but the provided a posteriori variance.

The two problems arising from this effect are: first, validation procedures using the a posteriori variance (e.g. ADOP tests) are returning too optimistic success rates, second, the combination of different estimates having different correlation times result in severe mis-weighting, e.g. between code and carrier observations.

## FAMCAR OBSERVABLES AND FILTERS

As a starting point, per carrier-frequency two observables are available: Carrier phase and pseudorange. So in principle, for  $n$  carrier frequencies, it should be possible to design  $2n$  separate filters. An observable combination  $comb$  can be defined in terms of the carrier and code coefficients  $\vec{a}_{comb}$  and  $\vec{b}_{comb}$ .

$$l_{comb} = \vec{a}_{comb}^T \cdot \begin{pmatrix} \phi_1 \\ \vdots \\ \phi_{nf} \end{pmatrix} + \vec{b}_{comb}^T \cdot \begin{pmatrix} \rho_1 \\ \vdots \\ \rho_{nf} \end{pmatrix}$$

Here,  $\phi_i$  denotes the  $i^{\text{th}}$  carrier phase observable and  $\rho_i$  the  $i^{\text{th}}$  code observable.

All carrier phase combinations are characterized by:

$$\vec{b}_{phase} = \begin{pmatrix} b_1 \\ \vdots \\ b_{nf} \end{pmatrix} = \vec{0}$$

The combinations constructed are the following:

### Minimum-error geometric carrier phase

The “geometric” condition is defined as follows:

$$geo(\vec{a}_{geo}, \vec{b}_{geo}) = \begin{pmatrix} 1 & \dots & 1 \\ \lambda_1 & \dots & \lambda_{nf} \end{pmatrix} \cdot \vec{a}_{geo} + (1 \quad \dots \quad 1) \cdot \vec{b}_{geo} = 1$$

In addition, the total error (also including ionospheric residual) is minimized (see also [Sjöberg 1990]). The resulting carrier phase observable is used in a conventional floating solution geometric filter. Optimally, this filter models temporally correlated errors in the combination from residual ionosphere and multipath.

### Minimum-error ionospheric geo-free carrier phase

For this combination, the “geometry-free” condition must be met:

$$iono(\vec{a}_{iono}, \vec{b}_{iono}) = \begin{pmatrix} 1 & \dots & 1 \\ \lambda_1 & \dots & \lambda_{nf} \end{pmatrix} \cdot \vec{a}_{iono} + (1 \quad \dots \quad 1) \cdot \vec{b}_{iono} = 0$$

Also, the combination must contain the full ionospheric residual, making the combination “ionospheric”:

$$iono(\vec{a}_{iono}, \vec{b}_{iono}) = \begin{pmatrix} -\lambda_1 & \dots & -\lambda_{nf} \\ \lambda_1^2 & \dots & \lambda_{nf}^2 \end{pmatrix} \cdot \vec{a}_{iono} + \begin{pmatrix} \lambda_1^2 & \dots & \lambda_{nf}^2 \\ \lambda_1^2 & \dots & \lambda_{nf}^2 \end{pmatrix} \cdot \vec{b}_{iono} = 1$$

For more than two carriers, additional degrees of freedom are available for the combination, enabling to define a minimum-error geometry-free ionospheric combination (see below).

### Geometry-free and ionosphere-free

For complete use of the carrier phase information, only two combinations have been considered so far. For  $nf$  carriers, this leaves  $nf-2$  independent carrier combinations to define. These additional combinations are geometry-free and ionosphere-free:

$$geo(\vec{a}_{Q_k}, \vec{b}_{Q_k}) = \begin{pmatrix} 1 & \dots & 1 \\ \lambda_1 & \dots & \lambda_{nf} \end{pmatrix} \cdot \vec{a}_{Q_k} + (1 \quad \dots \quad 1) \cdot \vec{b}_{Q_k} = 0$$

$$iono(\vec{a}_{Q_k}, \vec{b}_{Q_k}) = \begin{pmatrix} -\lambda_1 & \dots & -\lambda_{nf} \\ \lambda_1^2 & \dots & \lambda_{nf}^2 \end{pmatrix} \cdot \vec{a}_{Q_k} + \begin{pmatrix} \lambda_1^2 & \dots & \lambda_{nf}^2 \\ \lambda_1^2 & \dots & \lambda_{nf}^2 \end{pmatrix} \cdot \vec{b}_{Q_k} = 0$$

Due to this nature of being free from geometry, clock, troposphere and ionosphere errors, they are called *Quintessence* combinations (see [Paracelsus]).

For more than three carriers multiple independent Quintessence combinations are possible.

### Geometry-free and ionosphere-free code-carrier

To use the code information, for every carrier frequency  $k$  a code-carrier combination is defined using exactly one original code observation.

$$\vec{b}_{CC_k} = \begin{pmatrix} 0 \\ \vdots \\ 0 \\ 1 \\ 0 \\ \vdots \\ 0 \end{pmatrix}$$

The complete combination is again defined geometry-free and ionosphere-free:

$$geo(\vec{a}_{CC_k}, \vec{b}_{CC_k}) = \left( \frac{1}{\lambda_1} \quad \dots \quad \frac{1}{\lambda_{nf}} \right) \cdot \vec{a}_{CC_k} + (1 \quad \dots \quad 1) \cdot \vec{b}_{CC_k} = 0$$

$$iono(\vec{a}_{CC_k}, \vec{b}_{CC_k}) = \left( -\frac{\lambda_1}{\lambda_1^2} \quad \dots \quad -\frac{\lambda_{nf}}{\lambda_1^2} \right) \cdot \vec{a}_{CC_k} + \left( \frac{\lambda_1^2}{\lambda_1^2} \quad \dots \quad \frac{\lambda_{nf}^2}{\lambda_1^2} \right) \cdot \vec{b}_{CC_k} = 0$$

Additional degrees of freedom can be satisfied applying a minimum error condition concerning the carrier phase combination (see below).

All geometry-free observable combinations are filtered with a simple filter minimally modeling the ambiguity, optimally modeling the temporally correlated remaining errors.

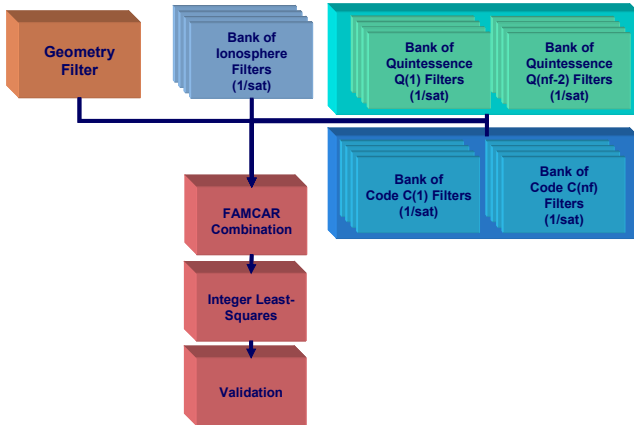


Figure 5: Full FAMCAR process

In Figure 5 the complete FAMCAR filter setup is shown. It consists of one geometry filter, a bank of ionosphere filters (1 per satellite), a set of  $nf-2$  banks of Quintessence filters and a set of  $nf$  banks of code-carrier filters.

### FAMCAR COMBINATION

The combinations defined before each observe and ambiguity combination defined by the carrier coefficients. To retrieve the complete solution for all satellites and all original carrier frequencies, a least-squares adjustment of the individual filter results is performed:

$$\vec{x}_{comb} = Q_{comb} \cdot \left( \vec{a}_{geo} \cdot Q_{geo}^{-1} \cdot \vec{x}_{geo}^T + \vec{a}_{iono} \cdot Q_{iono}^{-1} \cdot \vec{x}_{iono}^T + \sum_{k=1}^{nf} \vec{a}_{cc_k} \cdot Q_{cc_k}^{-1} \cdot \vec{x}_{cc_k}^T + \sum_{k=1}^{nf-2} \vec{a}_{Q_k} \cdot Q_{Q_k}^{-1} \cdot \vec{x}_{Q_k}^T \right)^{-1}$$

$$Q_{comb} = \left( \vec{a}_{geo} \cdot Q_{geo}^{-1} \cdot \vec{a}_{geo}^T + \vec{a}_{iono} \cdot Q_{iono}^{-1} \cdot \vec{a}_{iono}^T + \sum_{k=1}^{nf} \vec{a}_{cc_k} \cdot Q_{cc_k}^{-1} \cdot \vec{a}_{cc_k}^T + \sum_{k=1}^{nf-2} \vec{a}_{Q_k} \cdot Q_{Q_k}^{-1} \cdot \vec{a}_{Q_k}^T \right)^{-1}$$

with float solutions  $\vec{x}_p$ , covariance matrices  $Q_p$  and carrier phase coefficients  $\vec{a}_p$  for observable combination  $p \in \{geo, iono, cc_k, Q_k\}$ .

The resulting floating solution  $\vec{x}_{comb}$  and covariance matrix  $Q_{comb}$  is finally processed by integer least squares (e.g. LAMBDA) and established validation procedures to retrieve the best solution and its probability of correctness.

### STATISTICAL PROPERTIES

The set-up of the observables handled by the FAMCAR filters has the following important properties, justifying the whole approach. To present them, a covariance analysis has to be performed.

First an augmented coefficient vector is defined:

$$\vec{c} = \begin{pmatrix} a_1 \\ \vdots \\ a_{nf} \\ b_1 \\ \vdots \\ b_{nf} \\ f_{iono} \end{pmatrix} = \begin{pmatrix} 1 & \dots & 0 \\ \vdots & \ddots & \vdots \\ 0 & \dots & 1 \\ 0 & \dots & 0 \\ \vdots & \ddots & \vdots \\ 0 & \dots & 0 \\ -\frac{\lambda_1}{\lambda_1^2} & \dots & -\frac{\lambda_{nf}}{\lambda_1^2} \end{pmatrix} \cdot \vec{a} + \begin{pmatrix} 0 & \dots & 0 \\ \vdots & \ddots & \vdots \\ 0 & \dots & 0 \\ 1 & \dots & 0 \\ \vdots & \ddots & \vdots \\ 0 & \dots & 1 \\ \frac{\lambda_1^2}{\lambda_1^2} & \dots & -\frac{\lambda_{nf}^2}{\lambda_1^2} \end{pmatrix} \cdot \vec{b}$$

This coefficient vector contains carrier and code coefficients together with a last one defining the resulting ionospheric residual in the combined observable. The complete covariance matrix for carrier, code and ionospheric residual variances can be defined as

$$Q = \begin{pmatrix} \sigma\phi_1^2 & 0 & \dots & 0 \\ 0 & \ddots & & \\ \vdots & & \sigma\phi_{nf}^2 & \\ & & & \sigma\rho_1^2 & \\ & & & & \ddots & \\ 0 & & & & & \sigma\rho_{nf}^2 & 0 \\ & & & & & 0 & \sigma_{iono}^2 \end{pmatrix}$$

with the carrier phase variance  $\sigma\phi_i^2$  for the  $i^{\text{th}}$  carrier,  $\sigma\rho_i^2$  for the  $i^{\text{th}}$  code and  $\sigma_{iono}^2$  for the variance of the ionospheric residual. Please note that no covariance between frequencies have been accounted for. Though – due to the L2 tracking techniques implemented – there is some correlation between L1 and L2 for typical GPS data, this correlation is limited to the noise component and is neglectable at

everything but zero-baselines. For Galileo and modernized GPS, no such correlation effect is to be expected. In principle, they could be included in the formulas.

Now the total error of an observable combination  $\vec{c}$  can be determined:

$$\sigma^2(\vec{c}) = \vec{c}^T \cdot Q \cdot \vec{c}$$

This is the value minimized for any of the minimum-error combinations. Also, the covariance between two combinations  $\vec{c}_1$  and  $\vec{c}_2$  is computed as:

$$\sigma(\vec{c}_1, \vec{c}_2) = \vec{c}_1^T \cdot Q \cdot \vec{c}_2$$

For the first FAMCAR algorithm, it has already been shown that the minimum-error carrier phase combination and any geometry-free observable are uncorrelated. It can be shown similarly that the minimum-error ionospheric combination and any geometry- and ionosphere-free combination are uncorrelated, too (the lengthy proof is beyond the scope of this paper).

For the code-carrier combinations, “practically” uncorrelated observable combinations are defined. Considering the fact that the code error variance is orders of magnitude higher than the carrier phase variances, only the code variances have to be accounted for. This results in a neglectable correlation with the carrier phase combinations. In addition, the code-carrier combinations are ionosphere and geometry free and constructed from one code observation each. This creates them uncorrelated with each other. Though it should be possible to design truly uncorrelated observable combinations here, the additional complication is by far outweighing the benefits of a theoretically “more clean” solution.

$$\sigma(\vec{c}_1, \vec{c}_2) = \vec{c}_1^T \cdot Q \cdot \vec{c}_2 = 0$$

### COMPUTATIONAL DEMANDS

The least-squares filtering method is fundamentally of cubic order with respect to the number of states modeled. For this comparison, the full filter solution has position and receiver clock error states, ionosphere states per satellite and ambiguity and code and carrier multipath states per satellite per frequency. The FAMCAR geometry filter has position and receiver clock error states, one ambiguity and one carrier multipath/iono state per satellite. The geometry-free filters are all simple scalar filters.

The following table gives some examples of the load and the improvement factor of FAMCAR over the full filter formulation.

No. Satellites	Improvement 2 freq	Improvement 3 freq	Improvement 4 freq
5	31	94	212

6	34	106	240
7	37	115	264
8	39	124	284
9	41	131	302
10	43	137	317

To present the FAMCAR technique as an enabling method for improved processing, the following table is given. It shows the complexity of the simple modeling case for the full filters versus the complete modeling in FAMCAR.

No. Satellites	Improvement 2 freq	Improvement 3 freq	Improvement 4 freq
5	0.5	1.2	2.5
6	0.5	1.4	2.9
7	0.6	1.6	3.3
8	0.6	1.7	3.7
9	0.6	1.8	4.0
10	0.7	1.9	4.3

For two frequencies, the transition to full modeling has only a small impact if using FAMCAR instead of the full filter approach. For three and four frequencies, even a speed improvement will be implemented.

### SUMMARY

FAMCAR is mainly a very efficient method for computing a floating solution for multiple carrier signals in order to provide a powerful yet computationally low profile solution. As the modeling of temporal correlations has a much smaller impact on the processing demands than for classical “big filter” approaches, this qualifies FAMCAR as an enabling technique for complete modeling of errors. This is even truer the more carrier frequencies are available.

The presented FAMCAR technique has been filed for an U.S. patent.

### REFERENCES

- Carlsson, N.A. (1990):** *Federated Square Root Filter for Decentralized Parallel Processing*, IEEE Transactions on Aerospace and Electronic Systems, Vol.AES-26, No.3, May 1990
- Cliatt, S., (2003):** *GPS Modernization*, Proceedings of the GNSS 2003, April 22-25 2003, Graz, Austria.
- de Jonge, P., Tiberius, C (1996):** *The LAMBDA method for integer ambiguity estimation: implementation aspects*, Publications of the Delft Geodetic Computing Centre, LGR Series, No. 12, August 1996
- Forsell, B., Martin-Neira, M., Harris, R.A. (1997):** *Carrier Phase Ambiguity Resolution in GNSS-2*, Proceedings of the ION GPS-97, Kansas City, September 16-19, 1997, pp. 1727-1736.
- Harris, R.A. (1997):** *Direct Resolution of Carrier-Phase Ambiguity by “Bridging the Wavelength Gap”*,

ESATEC internal report TST/60107/RAH/Word; 03/02/97.

**Hein, G., Godet, J., Issler, J.-L., Martin, J.-C., Erhard, P., Lucas, R., Pratt, T. (2003):** *Galileo Frequency & Signal Design*, GPS World, June 2003, pp. 30-37.

**Hernández-Pajares, M., Juan, J.M., Sanz, J., Colombo, O.L. (2003):** *Impact of Real-Time Ionospheric Determination on Improving Precise Navigation with Galileo and Next-Generation GPS*, navigation Vol. 50, No. 3, Fall 2003, pp. 205-218.

**Joosten, P., Teunissen, P. J. G., Jonkman, Niels (1999):** *GNSS Three Carrier Phase Ambiguity Resolution using the LAMBDA-method*, Proceedings of the GNSS 1999

**Paracelsus – Ph. Theophrastus Bombastus von Hohenheim (1493\*-1541<sup>†</sup>):** *The Book Concerning The Tincture Of The Philosopher.*

**Sauer, K., Vollath, U., Amarillo, F. (2004):** *Three and Four Carriers for Reliable Ambiguity Resolution*, Proceedings of the ENC-GNSS 2004, Rotterdam, Netherlands (to be published).

**Sjöberg, L. E. (1990):** *The best linear combinations of L1 and L2 frequency observables in the application of Transit/Doppler and GPS*, manuscripta geodetica (1990) 15: pp. 17-22.

**Teunissen, P.J.G. (1995):** *The least-squares ambiguity decorrelation adjustment: a method for fast GPS integer ambiguity estimation*, Journal of Geodesy, 1-2, pp. 65-82.

**Teunissen, P.G., Tiberius, C. C. J. M. (1994):** *Integer least-squares estimation of the GPS phase ambiguities*. Proceedings of the KIS 1994

**Teunissen, P.G., Odijk, D.. (1997):** *Ambiguity dilution of precision: Definition, Properties and Application*, Proceedings of the ION GPS-97, 16-19 September, Kansas City, USA, pp. 891-899

**Teunissen, P.G. (1998):** *Success probability of integer ambiguity rounding and bootstrapping*, Journal of Geodesy (1998) 72, pp. 606-612.

**Vollath, U., Birnbach, S., Landau, H., Fraile-Ordonez, J. (1998):** *Analysis of Three-Carrier Ambiguity Resolution (TCAR) Technique for Precise Relative Positioning in GNSS-2*, Proceedings of the ION-GPS 1998

**Vollath, U., Roy. E. (2001) I:** *Ambiguity Resolution using Three Carriers, Performance Analysis using "Real" Data*, Proceedings of the GNSS-2001 conference.

**Vollath, U., Roy. E. (2001) II:** *Laboratory Experiment On Carrier Phase Positioning Techniques for GNSS-2 (TCAR-Test) Final Report*, ESA ESTEC, Contract number 12.406/77/NL/DS Rider 1

**Vollath, U., Landau, H., Chen, X., Doucet, K., Pagels, C. (2002):** *Network RTK Versus Single Base RTK - Understanding the Error Characteristics*, Proceedings of the GNSS-2002 conference, pp. 2774-2780

**Vollath, U., Sauer, K., Amarillo, F., Pereira, J.(2003):** *Three or Four Carrier- How Many are Enough?*, Proceedings of the ION-GPS 2003.

**Wang, J., Stewart, M.P., Tsakiri, M. (1998):** *A discrimination procedure for ambiguity resolution on-the-fly*, Journal of Geodesy (1998) 72, pp. 644-653.